Yahia ACHOUR [1], Jacek STARZYŃSKI[1], Adam JÓŚKO[2], Marek SUPRONIUK[1]

Military University of Technology, Faculty of Electronics (1), Warsaw University of Technology, Faculty of Electrical Engineering (2)

doi:10.15199/48.2019.11.29

D-dot, B-dot Data Processing of Fields Generated with Broadband Pulsed Antenna

Abstract. *This paper describes the measurement of both electric and magnetic fields generated by a broadband antenna feed with high voltage pulse generator. Data from both D-dot and B-dot sensors are collected at some distances from the antenna to investigate building up of the far field radiation. The paper discusses the problem of how to treat the irregular signals obtained from the probes and how to handle the time shifting caused by the different delay created by the sensors and the optical transmission. The obtained results are compared with those obtained from the simulation of the system using ANSYS-HFSS software.*

Streszczenie*. W artykule przedstawiona została metoda analizy danych z sond pola elektrycznego (D-dot) i magnetycznego (B-dot) w celu skorelowania pomiarów i oceny pasma i efektywności radiacji anteny szerokopasmowej podłączonej do generatora impulsów wysokiego napięcia. Wyniki pomiarów są rejestrowane w różnych odległościach od anteny w celu zbadania procesu formowania dalekiego pola anteny. W pracy omówiono zagadnienia związane z analizą nieregularnych sygnałów pomiarowych oraz wpływem przesunięć czasowych generowanych zarówno przez czujniki jak i optyczną transmisję sygnałów na wyniki analizy. Uzyskane wyniki pomiarów są porównywane z wynikami symulacji systemu przy użyciu oprogramowania ANSYS-HFSS. (**Obróbka danych z sond B-dot oraz D-dot dla pola szerokopasmowej anteny impulsowej**).*

Keywords: Pulse generator; Broadband antenna; Field measurement.
Słowa kluczowe: impulsy elektromagnetyczne, pomiar pola, antena szerokopasmowa.

Introduction

During our attempt to build a jamming system based on electromagnetic pulse (EMP) system [1], we had to measure the radiated electrical and the magnetic fields using fast D-dot and B-dot probes [2]. These measurements were necessary to confirm that the jammer is really radiating and also to get more information about the frequency range and the power density of the generated waves.

After recording data, we faced two major problems. The first one is that the two curves do not start at the same time. This difference is caused by the delay in the optical links which are not the same for both sensors and additionally by the propagation time in the conditioning circuit. The second problem was to find the ratio between the two signals, because the irregular form of the signals made it difficult to describe them in a parametrized form.

The first problem was solved with calculating and maximizing the correlation between the two. The second issue was approached as a single variable optimization problem, in which we tried to minimize the distance between the electrical field data and the magnetic field data. If there is a propagation, this optimization variable would fit to the intrinsic impedance of the air for the far field mode. Recording data at different distances from the antenna allowed us to analyze the attenuation of the near field static component and the building up of the far field.

Description of the EMP generator and the measurement setup

The experimental setup consists of two main parts: a high voltage pulse generator connected directly to a broadband antenna, which contains the Electromagnetic pulse (EMP) generator, or in other words, the jammer. In the second part, the radiated field is sensed and recorded via free field D-dot and a B-dot probes located nearby the antenna. The probes are connected to fast oscilloscope with a 40 GS per second using an optical link. The oscilloscope is located inside a shielded container in order to protect it from any electromagnetic wave and also to reject any possible perturbation and noises in the recorded signals. The distance between the antenna and the probes is changed from 25 cm to 7 m in order to check the influence of the distance on the radiated field and also to validate that the wave is propagating and to calculate the Factor of Merit (FoM) of the jammer. FoM, expressed in volts, is a popular factor used to describe efficiency of the radiating source of disturbances. It is defined as the product of the peak to peak amplitude of the electric field times the distance at which the field is recorded. For example, a device giving peak magnitude of 30 V/m at 100 meters from the antenna will have FoM = 30 V/m • 50 m = 1500 V.

The used high voltage pulse generator shown in figure 1 is a three stages Marx generator with inductive charging. In such a structure, the resistors used in classical Marx generator are replaced by coupled inductors. This technique allows getting the high repetition rate needed in the jamming system because the efficiency of the jammer is proportional to the total radiation time in one second which is in fact the product of the pulse width times the repetition rate. In next design of the generator we plan to use a solid-state solution such as transistors or photoconductive semiconductor switch (PCSS) [3, 4].

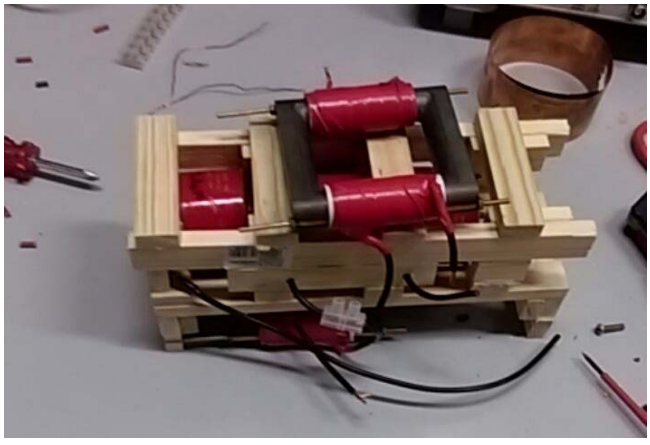

Fig 1: Pulse generator

Due to the compact structure of the high voltage pulse generator, its resulting parasitic inductance is very low. In this way, we were able to get fast pulses with a rise time in the range of nanosecond [5]. The rise time and the pulse width of the generated pulses are key-factors for better

radiation efficiency and to reach the radiation bandwidth of the antenna.

A bi-conical dipole antenna, shown in figure 2 was used in the presented prototype. This type of antenna is very popular in pulsed power field in order to create broadband radiation or electromagnetic pulse (EMP) [6]. The measured characteristics of the impedance magnitude and phase, using a network analyzer, are shown in figure 3. From these charts we can predict the auto-resonance frequencies of the antenna which corresponds in fact to the frequencies that the antenna will radiate as a response to a short enough pulse excitation. A list of first four lowest resonant frequencies of the used antenna are given in table 1 with the corresponding impedance.

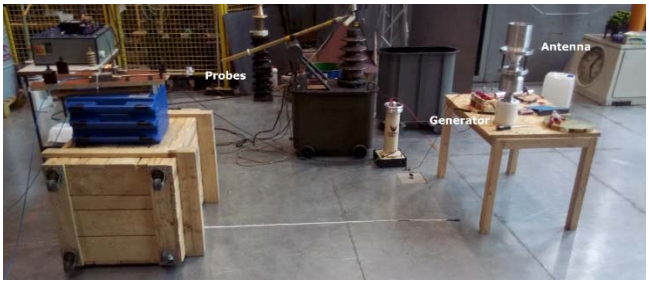

Fig 2: Measurement Setup

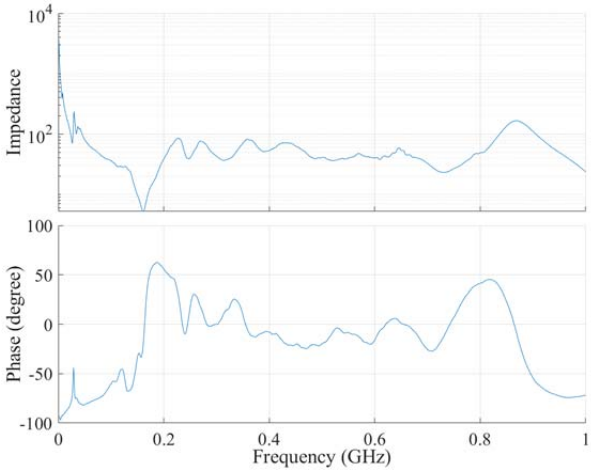

Fig 3: Spectrum of the antenna impedance

According to Dirac and Fourier theories, these frequencies are the resonant values in which the antenna oscillates if it is exited with a perfect pulse. However, in practice, a perfect Dirac pulse cannot be achieved. That's why it is necessary to study the influence of the rise time of the pulse of the radiation of the antenna.

Table 1: Measured resonant frequencies with the corresponding impedance

Frequency [MHz]	Impedance magnitude [Ω]
161	5.22
248	38.94
313	36.68
391	51.1

In order to do so, a finite element (FE) model of the antenna was implemented in ANSYS-HFSS software. This simulation was elaborated to investigate the influence of the switching time of the high voltage pulse generator on the FoM. The results, shown in table 2, were obtained by feeding the antenna with a 21 kV pulse in order to be close to the real system. However, we were not able to perform this test experimentally because the rise time of the pulse generator is not controllable (which is the case for almost all pulse generators), It depends on the dynamics of the used switches and the geometry of the generator.

Table 2: FoM as a function of the switching time

Risetime (ns)	FoM (kV)
0.5	7.5
1	5
1.5	3.5
2	2.8
2.5	2.4

After firing the real pulse generator, the recorded signals are shown in figure 4. The red (C2) and blue (C3) signals are directly recorded from the free field D-dot and B-dot probes respectively. They represent the time derivatives of the two fields. The reconstructed fields' waveforms are shown in pink and light blue (F2) and (F3).

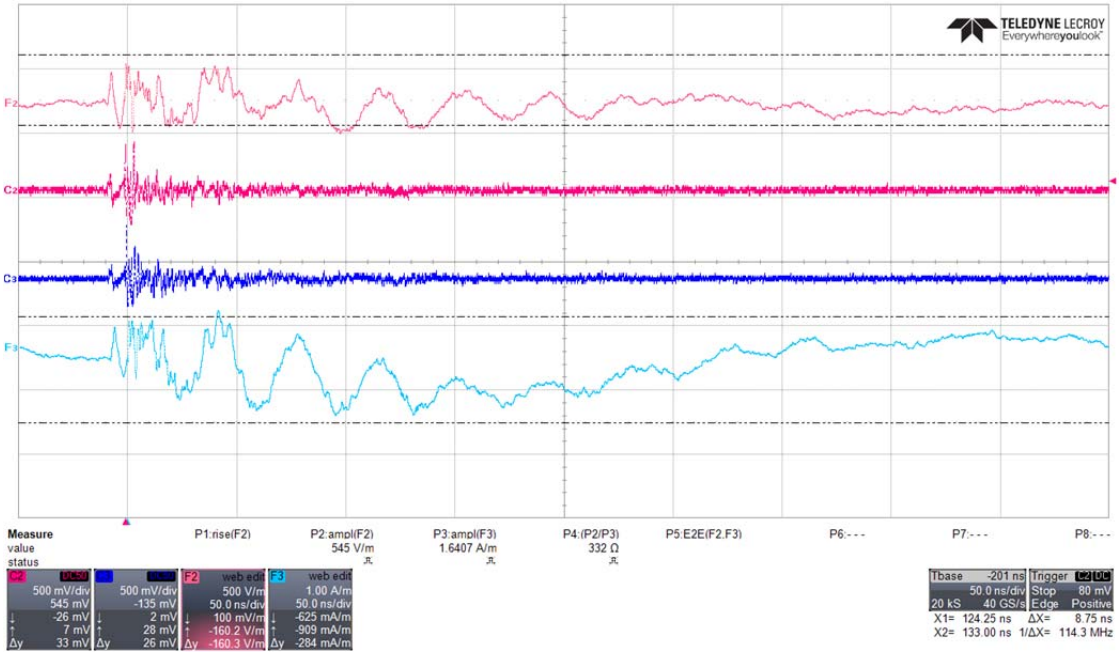

Fig. 4: Recorded signals at 3.5m from the antenna

Estimation of the delay between the two signals

As we mentioned previously, the two recorded signals have a time delay between them caused by the different lengths of the optical fibers and also by the propagation time within the conditioning circuit.

In order to estimate this delay, the correlation between the two signals were calculated as shown in figure 5. From this waveform, we can notice clearly that the correlation function has one peak which corresponds to the best (almost ideal) fitting of the two curves. The corresponding delay between the two signals is estimated here to be 9.5 ns for signals recorded at 3.5 m from the antenna. For the last part of this paper, all the recorded signals will be shifted by the calculated delay in order to restore the same time origin for both signals.

We should mention that the correlation waveform, shown in figure 5, is normalized with dividing it by its maximal value. This was done for better visualization and to get more consistent idea about the magnitude of the function compared to the peak value.

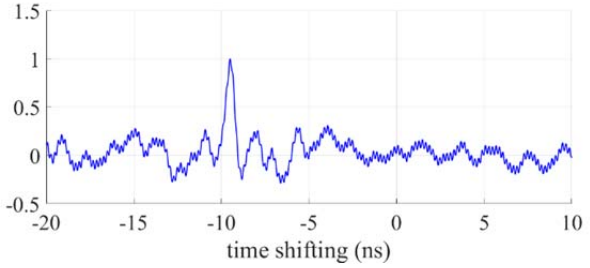

Fig. 5: Normalized correlation between the electric and magnetic fields for time window in range -20 to 10 ns

E/B ratio estimation

As we can see from figure 4, the radiated fields have very irregular waveforms. Thus, it is difficult to find the ratio between them which represents intrinsic impedance of air which should be in the ideal case 377 Ω.

However, in our case, the fields are measured nearby the antenna which means that we are measuring the superposition of the near and the far fields components. Moving far away from the antenna, the near field vanishes, and the far field builds up continues propagation.

Knowing that our radiation is initially caused by the voltage applied to the antenna, then next to the antenna, the electric field is high, however, the magnetic field is not developed yet. This means that the measured ratio between the two fields (E/H) should be bigger than the intrinsic impedance for the far field. Moving away from the antenna, this ratio decreases due to the induced magnetic field created by the variation of the electrical one.

In order to estimate E/H ratio, we adopted a technique based on an optimization process which tries to minimize the distance between the two curves by acting on this ratio. The value which corresponds to the minimum distance is then considered as the best estimation of the ratio. The objective function is calculated as

$$f(z) = \frac{1}{N}\sum_{k=1}^{N}\left(\frac{E_k}{z} - H_k\right)^2, \tag{1}$$

where E_k and H_k are the electric and magnetic field samples, N is the number of registered samples and z is the design parameter, optimal value of which can be associated with the intrinsic impedance Z. An example of objective function curve (for measurements taken at 3.5 m from the antenna) and its optimum is shown in figure 6.

In the classical case the optimum of this function can be calculated exactly and directly by the differentiation according to "z" of the $f(z)$ function. This will lead to the following equation

$$z_{opt} = (\boldsymbol{E}^T \cdot \boldsymbol{H})^{-1} \cdot \boldsymbol{E}^T \cdot \boldsymbol{E}, \tag{2}$$

where E and H are column vectors containing all the E_k and H_k samples. In fact, this is true only if we assume that z is constant. However, this is not completely true in our situation because the studied signal is superposition of many harmonics with different frequencies, thus different wavelengths. This means that the far field border for each frequency can differ from the others. Following this path, we can deduce that the assumption of a constant impedance is not rigorous. For that reason, we have developed the optimization framework to be used in future for more complex models of the impedance. But in this paper, as a test, we are considering the simplest case of a constant impedance. The obtained results shown in figure 6 and table 3 are equivalent to those obtained using the previous expression.

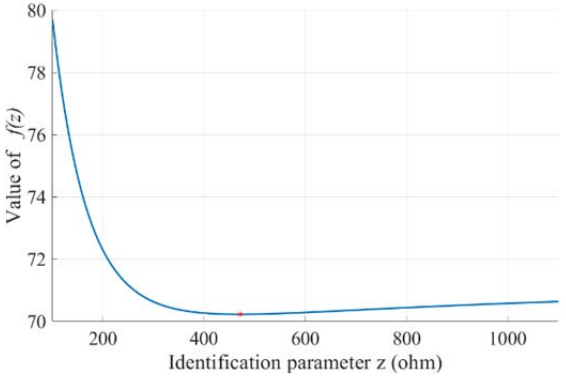

Fig. 6: Example objective function $f(z)$ at 3.5 m distance from the antenna; the minimum is marked with a red dot

a)

b)

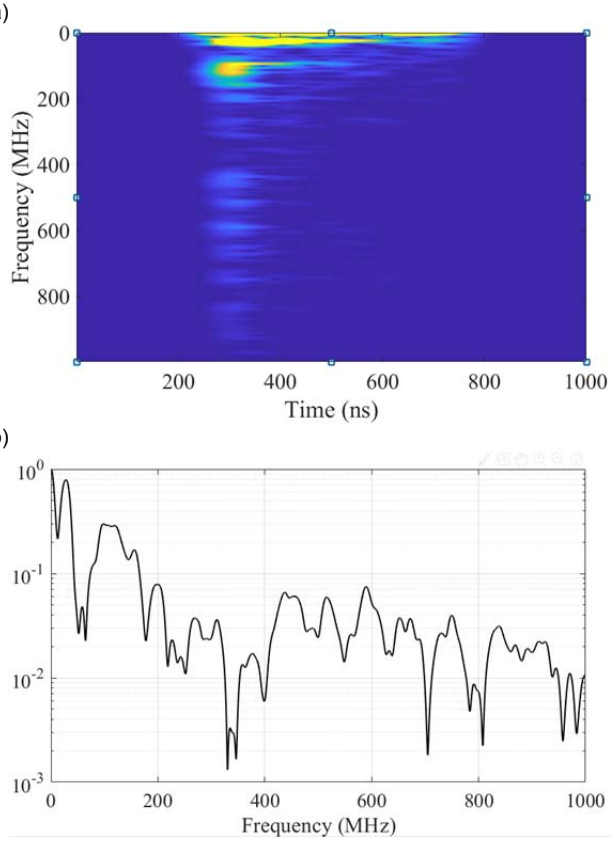

Fig. 7. Time frequency analysis of the radiated electric field at 3.5 m from the antenna a) and signal spectrum at time 300 ns b).

This operation was repeated for a number of distances from the antenna, the obtained results are presented in table 3. These values are the average value for 10 measurements at each distance.

Table 3: Effective intrinsic impedance at different distances from the antenna

Distance (cm)	E/H (Ω)	FoM (V)
25	1192	1224
175	509	980
350	471	823
700	463	776

Time frequency analysis

In order to understand how the antenna is radiating and which frequencies it contains, a time-frequency analysis was applied on the recorded signal as shown in figure 7.

From figure 7 we can notice that the antenna is effectively radiating at several frequencies which almost exactly corresponds to the resonant frequencies listed in table 1. The small differences are caused by the resolution of the FFT calculation because the duration of the signal is too short and also to the measurement errors.

Conclusions

The paper describes a data processing approach developed to analyze recorded signals obtained using two different free fields probes. The used techniques helped us to understand better the pulsed mode radiation of the broadband antenna and the mechanism of building-up the far field.

A jamming system, which consists of a high voltage pulse generator based on a three stages Marx structure inductively charged, was built and connected to a broadband dipole antenna. Both electric and magnetic fields were recorded at selected distances from the antenna. The obtained data was treated to and analyzed to extract several parameters such as the intrinsic impedance, the power density, and also the time variation spectrum of the generated pulses (see figure 7a). The obtained results allowed us to confirm that the system is working, and the radiated field is effectively propagating.

***Authors**: dr inż. Yachia Achour, Wojskowa Akademia Techniczna, Wydział Elektroniki, ul. gen. Sylwestra Kaliskiego 2, 00 – 908 Warszawa 49; E-mail: yahia.achour@wat.edu.pl; dr hab. inż. Jacek Starzyński, Wojskowa Akademia Techniczna, Wydział Elektroniki, ul. gen. Sylwestra Kaliskiego 2, 00 – 908 Warszawa 49, E-mail: jacek.starzynski@wat.edu.pl; dr inż. Adam Jośko, Politechnika Warszawska, Instytut Elektrotechniki Teoretycznej i Systemów Informacyjno-Pomiarowych, Pl. Politechniki 1, 00-661 Warszawa, E-mail: adam.josko@ee.pw.edu.pl; dr inż. Marek Suproniuk, Wojskowa Akademia Techniczna, Wydział Elektroniki, ul. gen. Sylwestra Kaliskiego 2, 00 – 908 Warszawa 49, E-mail: marek.suproniuk@wat.edu.pl;*

REFERENCES

1. Achour, Y., Starzyński, J., Jośko, A.: Nanosecond EMP simulator using a new high voltage pulse generator, Przeglad Elektrotechniczny, vol.10(1), pp.35--38, 2017,
2. Lasica, A., Jośko, A., Starzyński, J.: Indirect Method for Kilovolt Nanosecond Pulses Measurement, International Conference Computational Problems of Electrical Engineering (CPEE), doi: 10.1109/CPEE.2018.8506802, 2018.
3. E. Majda-Zdancewicz, M. Suproniuk, M. Pawłowski, M. Wierzbowski: Current state of photoconductive semiconductor switch egineering, Opto-Electronics Review, vol. 26, ss. 92 – 102, 2018,
4. M. Suproniuk, P. Kamiński, R. Kozłowski, M. Teodorczyk, A. Mirowska, E. Majda-Zdancewicz, M. Wierzbowski, K. Piwowarski, P. Paziewski, "Semi-insulating GaP as a material for manufacturing photoconductive semiconductor switches" Proc. SPIE 11055; 2019; doi: 10.1117/12.2524108
5. Mayes, J. R., Carey, W. J., Nunnally, W. C., Altgilbers, L.: Sub-Nanosecond Jitter Operation of Marx Generators, Pulsed Power Plasma Science PPPS, doi: 10.1109/PPPS.2001.1002135, 2001.
6. Pecquois, R., Pecastaing, L., Rivaletto, M., De Ferron, A. S., Vezinet, R.: MOUNA: An Autonomous, Compact, High-Power, and Wideband Electromagnetic Source Based on a Novel Resonant Pulsed Transformer, IEEE Transactions on Plasma Science, vol. 40, (5), pp. 1407--1415. doi: 10.1109/TPS.2012.2189138, May 2012.